Organic Electronics 13 (2012) 1602–1605

Contents lists available at SciVerse ScienceDirect

Organic Electronics

journal homepage: www.elsevier.com/locate/orgel

Distributed feedback lasing from thin organic crystal based on active waveguide grating structures

Ran Ding [a], Hong-Hua Fang [a], Ying Wang [a], Shi-Yang Lu [b], Xu-Lin Zhang [a], Lei Wang [a], Jing Feng [a,*], Qi-Dai Chen [a], Hong-Bo Sun [a,b,*]

[a] State Key Laboratory on Integrated Optoelectronics, College of Electronic Science and Engineering, Jilin University, 2699 Qianjin Street, Changchun 130012, People's Republic of China
[b] College of Physics, Jilin University, 119 Jiefang Road, Changchun 130023, People's Republic of China

ARTICLE INFO

Article history:
Received 23 February 2012
Received in revised form 5 April 2012
Accepted 8 April 2012
Available online 23 May 2012

Keywords:
Organic crystal
Organic laser
Distributed feedback
Interference lithography

ABSTRACT

A simple method has been proposed to fabricate active waveguide grating structures as distributed feedback configuration for organic crystal lasers. Organic single crystals, 2,5-bis(4-biphenyl)bithiophene (BP2T), act as both the gain medium and the waveguide. The distributed feedback structures are fabricated separately on top of crystals through interference lithography. The lasing emissions centered at 566 nm with FWHM of 1.1 nm have been observed when the pump intensity exceeds 19 μJ cm^{-2}. This method features simple, nondestructive, and it is expected to be applied in the electronically pumped laser devices.

1. Introduction

Organic single crystals have attracted great attention in the application of optoelectronic devices such as organic field-effect transistors (OFETs) [1,2], electroluminescence (EL) devices [3,4], photovoltaic cells [5], and optically pumped lasers [6] because of their excellent electronic and optical properties originating from the high order molecular packing, and high chemical purity [7]. Furthermore, organic single crystals constructed by π-conjugated oligomers have been demonstrated with high stimulated emission cross section and self-waveguide emission properties, which are promising for laser active materials [7–12]. However, the number of reports on laser devices based on the single crystals is limited [6,13]. An important requirement to achieve lasing action is the optical feedback in the device. Among a variety of resonator geometries, the use of a structured medium providing distributed feedback (DFB) along the direction of propagation by a periodic modulation of refractive index or gain is particularly effective [14–16]. In previous study, we have fabricated distributed feedback laser based on the thiophene/phenylene co-oligomers crystals where Bragg gratings can be directly written in the crystal. However, this may introduce the cracks in the crystals, and photodecomposition may occur in degree during the interactions with high power laser. Furthermore, the laser ablation results are strongly dependent on the species of crystal and crystal orientation. Thus, there strongly need a simple method while maintains the intrinsic properties of organic crystals.

In this work, we propose a DFB configuration of active waveguide grating structures for crystal lasers, where a typical light emitting crystal material is used as the active medium, and a photoresist grating is fabricated on top of the active waveguide by using interference lithography. Based on the laser configuration, the second order distributed feedback laser emission in the yellow–green (at

* Corresponding authors. Address: State Key Laboratory on Integrated Optoelectronics, College of Electronic Science and Engineering, Jilin University, 2699 Qianjin Street, Changchun 130012, People's Republic of China.
E-mail addresses: jingfeng@jlu.edu.cn (J. Feng), hbsun@jlu.edu.cn (H.-B. Sun).
URL: http://www.lasun-jlu.cn/index.php (J. Feng).

1566-1199/$ - see front matter © 2012 Elsevier B.V. All rights reserved.
http://dx.doi.org/10.1016/j.orgel.2012.04.022

wavelength of ~566 nm) is obtained with a full width at half maximum (FWHM) of 1.1 nm and a pump threshold of 19 μJ cm^{-2}. This kind of configuration is proposed to be of particular importance for the design of crystal lasers.

2. Experimental details

2.1. Materials and photophysical properties

The laser medium used in the experiment is crystals of 2,5-bis(4-biphenyl)bithiophene (BP2T) (see its structural formula in inset of Fig. 1(a)). The materials of BP2T were purchased from Lumtec Corp., and the methods for the synthesis and purification of the BP2T have been described elsewhere [18]. Thin crystal materials were prepared by physical vapor transport method according to previous report [17]. The photographs of crystals were taken by using widefield fluorescence microscopy on BK-FL4 fluorescence microscope. Their absorption spectra were recorded on a Shimadzu UV-2550 spectrophotometer and steady-state fluorescence spectra were measured by an AvaSpec-2048 optical fiber spectrometer.

2.2. Lasing characterization of DFB lasers

For lasing characterization, second harmonic generation (400 nm) of a regenerative amplifier (Spitfire, Spectra Physics) was used as optical pump source. The spot size of the pump laser beam focused on the samples by a convex lens was estimated to be about 0.7 mm in radius which was perpendicular to the sample and the pump energy was controlled by using a set of calibrated neutral density filters and measured by laser power meter (LP1, Sanwa). The emitted light was detected by the optical fiber and then dispersed to a monochromator equipped with a charge coupled device (CCD) detector (iDus, Andor).

3. Results and discussion

3.1. Design and theoretical modeling of DFB lasers

The crystal constitutes a high-quality waveguide, and bright yellow–green light emits from the edges, as shown in Fig. 1(b), indicating that most of photons are confined inner the crystal and transfer to the edge. The optical properties including UV–vis absorption, photoluminescence spectrum and amplified spontaneous emission (ASE) spectrum of BP2T crystal shown in the Fig. 1(c). The pink and the red curves are the photoluminescence and ASE spectra of BP2T crystals, both of which are centered on 566 nm. And the blue curve shows that the absorption spectrum of BP2T crystal. In order to avoid destruction of crystal structures, we adopted the configuration as shown in Fig. 2(a). The grating structures are fabricated separately on top of crystals, where the crystals perform as optical gain media and the grating structures are for the Bragg diffraction. To understand the eigen modes in this configuration, we use our home-generated finite-difference time-domain (FDTD) codes to calculate the distribution of the electromagnetic field. Briefly, we first apply the transfer

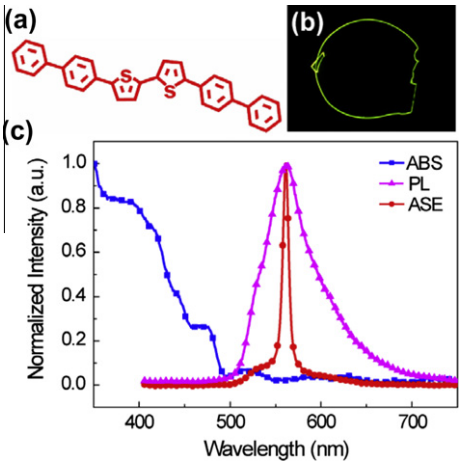

Fig. 1. (a) Chemical structure of BP2T. (b) Fluorescence photograph of BP2T crystal under the UV light irradiation. (c) The UV–vis absorption, photoluminescence spectrum and ASE spectrum of BP2T crystals.

matrix method to obtain the TM-polarized eigen field distribution in the crystal waveguide, which is set as the input source for the FDTD simulation. Then the periodic structure is modeled and a 10,000-steps FDTD simulation is performed, where the cell size is chosen as $\Delta s = 10$ nm, $\Delta t = 0.5\Delta s/c$ (free space light speed) and $\lambda = 566$ nm.

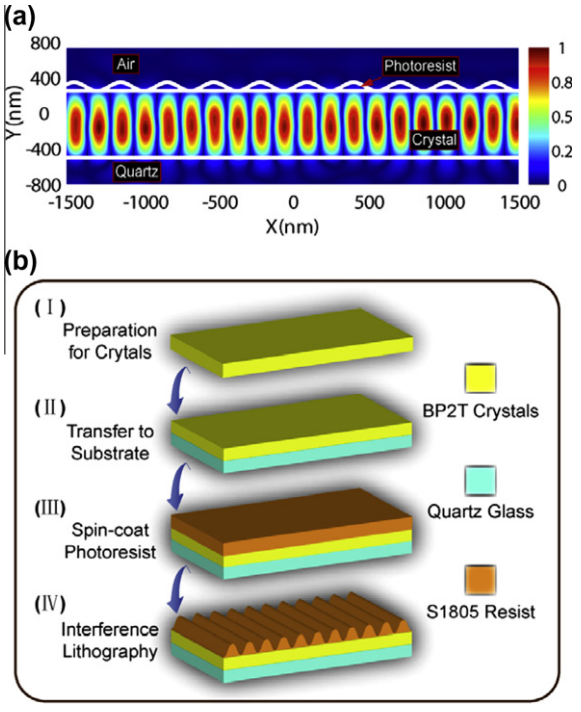

Fig. 2. (a) The eigen modes of the DFB laser devices. The color spots denote the TM-polarized eigen field distribution. (b) Scheme of fabrication of the grating on the crystal surface. The main fabrication process: growth of thin film single crystals, adhere crystals to the substrate, spin-coat S1805 photoresist on the surface of the crystals, UV laser interference lithography.

According to the simulation, the field distribution of the eigen mode is confined almost completely in the active waveguide layer which is shown in Fig. 2(a). This implies efficient utilization of the active volume and efficient extraction of the pump energy, as well as oscillation modes. In this simulation, the organic single crystal has a thickness of 800 nm, and the grating has a period of 320 nm and modulation depth of 100 nm. The substrate is assumed to be made of quartz and the medium on top of the laser device is air.

3.2. Fabrication and lasing performance of DFB lasers

To fabricate the organic single crystal laser, organic single crystal is firstly transported to the quartz substrate spin-coated with a film of NOA 61 (Norland Products) to adhere the crystal (Fig. 2(b)). Then S1805 photoresist (1:4, Shipley 1805/acetone) is spin-coated on the crystal surface at 3000 rpm, followed by a 60 s bake at 95 °C. Then the photoresist is exposed to a holographic grating pattern that is generated by interfering two beams from a continuous wave laser (266 nm, Coherent Inc). The photoresist located at the bright fringes of the interference pattern is exposed within about 800 ms. The periods (Λ) of the grating structures could be controlled by changing the angle θ between the two ultraviolet (UV) laser beams, according to: $\lambda = 2\Lambda\sin(\theta/2)$, where λ is the wavelength of the UV laser. The DFB laser devices with one-dimensional (1-D) periodic corrugation were fabricated according to the design. Scanning electron microscope (SEM) image of cross section of sample is shown in Fig. 3(a). Four layers: substrate, NOA 61, active BP2T crystal, and photoresist grating could be clearly observed. Since the refractive index ($n = 1.8$) of the crystal is higher than that of other layers ($n_{S1805} = 1.64$, $n_{NOA61} = 1.56$, $n_{quartz} = 1.45$), the emitted photons could be well restricted and waveguided in the crystal. The crystal would then act as both active medium and waveguide, while the photoresist grating performances as diffractive components. The atomic force microscope (AFM) topographic image of the grating is displayed in Fig. 3(b). The sample exhibits a feature height of ~100 nm with period of the grating of ~320 nm. Structures of higher aspect ratio can be obtained on crystals by increasing the explosion time and the thickness of S1805 controlled by the spin speed. Since the UV laser at low power was employed in lithography, no evident cracks were observed in the crystals, and it was also expected that no apparent photodecomposition during the fabrication process.

When increasing the pump energy above a certain threshold value, a narrow peak of FWHM less than 1.1 nm appears in the emission spectrum, and a coherent beam is emitted normal to the chipboard (Fig. 4(a)), indicating that laser action has begun. The photograph of Fig. 4(b) shows the photograph of the yellow–green emitting crystal laser, where the radiation pattern from the laser device consists of two opposite bright arcs. Fig. 5(a) shows the evolution of spectrum was recorded at room temperature for increasing pump fluence. The lasing wavelength is centered at 566 nm. It is noted that the emission is multimode. This may arise from the roughness of grating surface and the large thickness of crystal.

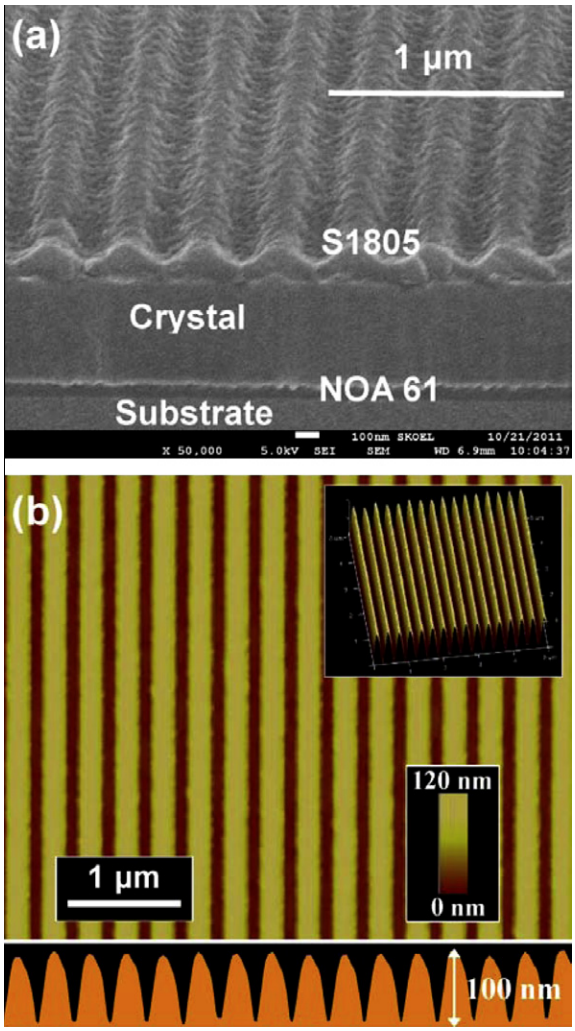

Fig. 3. (a) Image of device fabricated with 320 nm period grating on the surface of the crystals. (b) AFM image for the topographies of laser interference lithography of S1805 photoresist on top of the BP2T crystals.

Based on parameters mentioned above, including the central lasing peak wavelength ($\lambda_{em} = 566$ nm), the period of the grating ($\Lambda = 320$ nm), the refractive index n_{eff} (1.77) (calculated through a solution of the Helmholtz wave equation for a planar multilayer structure), and taking into account the Bragg expression [14] $m\lambda = 2n_{eff}\Lambda$, in which, the DFB device works at the second order of diffraction. Hence the DFB laser gets back-reflect due to Bragg scattering in a suitable periodic grating structure. And by taking advantages of a periodic change in refractive index, the DFB mechanisms reflect light in a waveguide to provide optical feedback. The emission peak intensity as a function of pump fluence is also plotted in Fig. 5(b) and shows a lasing threshold of about 19 μJ cm^{-2}, corresponding with 292 nJ pulse^{-1}. It is noted that the pump threshold of this laser is lower than that of our previous work (25 μJ cm^{-2}). Considering the absorption of S1805 at the pump wavelength (400 nm), about 10% pump laser loses, a lower threshold is expected in this DFB configuration.

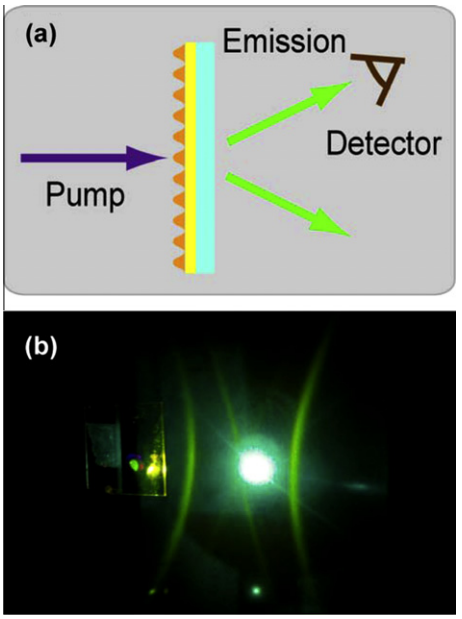

Fig. 4. (a) Scheme of pump laser beam and measured emission light direction. (b) The image of output laser emission from the laser device consists of two opposite bright arcs.

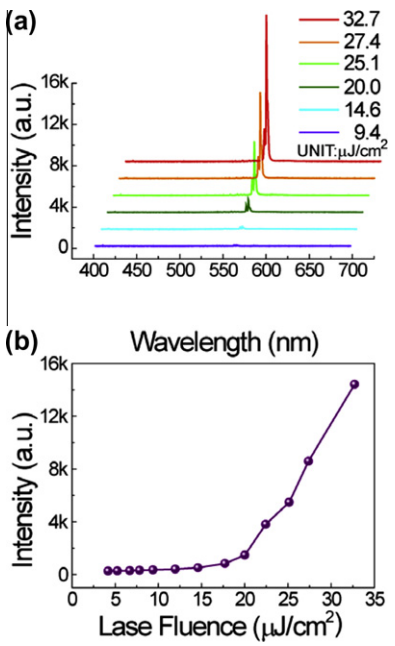

Fig. 5. (a) Measured spectra of the lasing emission of the laser at different pump intensity. (b) Emission dependence as a function of the pump intensity, indicating a pump threshold of about 19 μJ cm^{-2}.

In contract to the laser ablation method, the most important advantage of using this DFB configuration is that the Bragg gratings are fabricated on the crystal surface, and it does not need micromachining in the crystals [13]. This is crucial for the organic crystal devices, because the molecules hold together through van der Waals force in crystals, and they are generally fragile and difficult to handle. The avoidance of micromachining in the crystals may greatly maintain the intrinsic properties of crystal and improve the crystal device performance. Furthermore, fabrications of photoresist grating with small periods are much easier than that of directly writing microstructures in the crystals, and insensitive to the species of crystals.

4. Conclusions

In conclusion, organic crystal distributed feedback lasers have been fabricated by a simple method. The distributed feedback structures are fabricated separately on top of crystals through interference lithography. The second order distributed feedback lasing emission from the crystals has been realized. This method features simple, nondestructive, and may find great applications in crystal laser device.

Acknowledgements

The authors gratefully acknowledge the supports from National Basic Research Program of China (973 Program) under Grant No. 20l1CB013005, and from Natural Science Foundation of China (NSFC) under Grant Nos. 90923037 and 61107024. Hong-Hua Fang acknowledge the supports from Graduate Interdisciplinary Fund of Jilin University (No. 2011J008).

References

[1] C.L. Wang, X.M. Wang, J. Min, N. Zhao, J.B. Xu, Org. Electron. 12 (2011) 1731–1735.
[2] L. Jiang, W. Hu, Z. Wei, W. Xu, H. Meng, Adv. Mater. 21 (2009) 3649.
[3] Y.H. Chen, S.L. Lin, Y.C. Chang, Y.C. Chen, J.T. Lin, R.H. Lee, W.J. Kuo, R.J. Jeng, Org. Electron. 13 (2012) 43–52.
[4] Y. Bai, J. Feng, Y.F. Liu, J.F. Song, J. Simonen, Y. Jin, Q.D. Chen, J. Zi, H.B. Sun, Org. Electron. 12 (2011) 1927–1935.
[5] R.J. Tseng, R. Chan, V.C. Tung, Y. Yang, Adv. Mater. 20 (2008) 435.
[6] M. Ichikawa, R. Hibino, M. Inoue, T. Haritani, S. Hotta, K. Araki, T. Koyama, Y. Taniguchi, Adv. Mater. 17 (2005) 2073.
[7] H. Wang, F. Li, I. Ravia, B.R. Gao, Y.P. Li, V. Medvedev, H.B. Sun, N. Tessler, Y.G. Ma, Adv. Funct. Mater. 21 (2011) 3770.
[8] M. Polo, A. Camposeo, S. Tavazzi, L. Raimondo, P. Spearman, A. Papagni, R. Cingolani, D. Pisignano, Appl. Phys. Lett. 92 (2008) 3.
[9] W.J. Xie, Y.P. Li, F. Li, F.Z. Shen, Y.G. Ma, Appl. Phys. Lett. 90 (2007) 3.
[10] H.H. Fang, Q.D. Chen, J. Yang, H. Xia, B.R. Gao, J. Feng, Y.G. Ma, H.B. Sun, J. Phys. Chem. C 114 (2010) 11958.
[11] H.H. Fang, Q.D. Chen, J. Yang, H. Xia, Y.G. Ma, H.Y. Wang, H.B. Sun, Opt. Lett. 35 (2010) 441.
[12] H.H. Fang, B. Xu, Q.D. Chen, R. Ding, F.P. Chen, J. Yang, R. Wang, W.J. Tian, J. Feng, H.Y. Wang, H.B. Sun, IEEE J. Quantum Electron. 46 (2010) 1775.
[13] H.H. Fang, R. Ding, S.Y. Lu, J. Yang, X.L. Zhang, R. Yang, J. Feng, Q.D. Chen, J.F. Song, H.B. Sun, Adv. Funct. Mater. 22 (2012) 33.
[14] I.D.W. Samuel, G.A. Turnbull, Chem. Rev. 107 (2007) 1272.
[15] P. Gorrn, M. Lehnhardt, W. Kowalsky, T. Riedl, S. Wagner, Adv. Mater. 23 (2011) 869.
[16] G.A. Turnbull, P. Andrew, M.J. Jory, W.L. Barnes, I.D.W. Samuel, Phys. Rev. B 64 (2001) 125122.
[17] J. Yang, H.H. Fang, R. Ding, S.Y. Lu, Y.L. Zhang, Q.D. Chen, H.B. Sun, J. Phys. Chem. C 115 (2011) 9171.
[18] S. Hotta, H. Kimura, S.A. Lee, T. Tamaki, J. Heterocycl. Chem 37 (2000) 281.